doi:10.1093/brain/awl051 *Brain* (2006), **129**, 1113–1124

Functional connectivity of the fusiform gyrus during a face-matching task in subjects with mild cognitive impairment

A. L. W. Bokde,[1] P. Lopez-Bayo,[1] T. Meindl,[2] S. Pechler,[1] C. Born,[2] F. Faltraco,[1] S. J. Teipel,[1] H.-J. Möller[1] and H. Hampel[1]

[1]Dementia and Neuroimaging Research Section, Alzheimer Memorial Center and Geriatric Psychiatry Branch, Department of Psychiatry and [2]Department of Clinical Radiology, University Hospital of Munich, Ludwig-Maximilian University, Munich, Germany

Correspondence to: Arun L. W. Bokde, PhD, Dementia and Neuroimaging Research Section, Alzheimer Memorial Center and Geriatric Psychiatry Branch, Department of Psychiatry, Ludwig-Maximilian University, Nussbaumstrasse 7, 80336 Munich, Germany
E-mail: Arun.Bokde@med.uni-muenchen.de

Cognitive function requires a high level of functional interaction between regions of a network supporting cognition. Assuming that brain activation changes denote an advanced state of disease progression, changes in functional connectivity may precede changes in brain activation. The objective of this study was to investigate changes in functional connectivity of the right middle fusiform gyrus (FG) in subjects with mild cognitive impairment (MCI) during performance of a face-matching task. The right middle FG is a key area for processing face stimuli. Brain activity was measured using functional MRI. There were 16 MCI subjects and 19 age-matched healthy controls. The linear correlation coefficient was utilized as a measure of functional connectivity between the right middle FG and all other voxels in the brain. There were no statistical differences found in task performance or activation between groups. The right middle FG of the healthy control and MCI groups showed strong bilateral positive linear correlation with the visual cortex, inferior and superior parietal lobules, dorsolateral prefrontal cortex (DLPFC) and anterior cingulate. The healthy controls showed higher positive linear correlation of the right middle FG to the visual cortex, parietal lobes and right DLPFC than the MCI group, whereas the latter had higher positive linear correlation in the left cuneus. In the healthy controls, the right middle FG had negative linear correlation with right medial frontal gyrus and superior temporal gyrus and with left inferior parietal lobule (IPL), angular gyrus, superior frontal gyrus and anterior cingulate gyrus, but the MCI group had negative linear correlation with the left IPL, angular gyrus, precuneus, anterior cingulate, and to right middle temporal gyrus and posterior cingulate gyrus. In the negatively linearly correlated regions, the MCI group had reduced functional connectivity to the frontal areas, right superior temporal gyrus and left IPL. Different regions of the cuneus and IPL had increased functional connectivity in either group. The putative presence of Alzheimer's disease neuropathology in MCI affects functional connectivity from the right middle FG to the visual areas and medial frontal areas. In addition, higher linear correlation in the MCI group in the parietal lobe may indicate the initial appearance of compensatory processes. The results demonstrate that functional connectivity can be an effective marker for the detection of changes in brain function in MCI subjects.

Keywords: functional MRI; functional connectivity; object matching; visual system; face matching

Abbreviations: FG = fusiform gyrus; IPL = inferior parietal lobule; MCI = mild cognitive impairment

Received September 2, 2005. Revised January 30, 2006. Accepted February 3, 2006. Advance Access publication March 6, 2006

Introduction

Strategies for the early detection of the effects of Alzheimer's disease on brain function have relied primarily upon assessment of resting cerebral blood flow or glucose metabolism changes measured using PET (Azari *et al.*, 1993; Minoshima *et al.*, 1997; Caselli *et al.*, 1999; De Santi *et al.*, 2001; Reiman *et al.*, 2001; Alexander *et al.*, 2002; Herholz *et al.*, 2002;

Silverman *et al.*, 2002; Chetelat *et al.*, 2003; Grundman *et al.*, 2004; Reiman *et al.*, 2004) or on differences in activation due to a cognitive paradigm measured using PET or functional MRI (fMRI) (Pietrini *et al.*, 1996; Backman *et al.*, 2000; Bookheimer *et al.*, 2000; Rombouts *et al.*, 2000; Small *et al.*, 2000; Grady *et al.*, 2001, 2003; Greicius *et al.*, 2004; Rombouts *et al.*, 2005). There has been a more limited focus on utilizing the functional interactions between regions of a cognitive network as a possible marker for the detection of Alzheimer's disease (Azari *et al.*, 1993; Horwitz *et al.*, 1995; Grady *et al.*, 2001). In particular, Azari *et al.* (1993) found that the decrease in interactions between the frontal and parietal association cortices varied between healthy control subjects and mild to moderate stage Alzheimer's disease patients. Further supporting the breakdown in functional connections between frontal and posterior cortices, Grady *et al.* (2001) found that Alzheimer's disease patients had a functional disconnection between the prefrontal cortex and the hippocampus and suggested that memory breakdown early in the disease progression is related to a reduction in the integrated activity within a distributed network that includes these two areas. In addition, measurements of white matter tracts using diffusion tensor imaging showed structural changes in Alzheimer's disease patients compared with healthy controls (Rose *et al.*, 2000; Bozzali *et al.*, 2001; Bozzali *et al.*, 2002; Stahl *et al.*, 2003; Choi *et al.*, 2005). Alzheimer's disease patients showed a highly significant reduction in the integrity of the association white matter fibre tracts, such as the splenium of the corpus callosum, superior longitudinal fasciculus and cingulum (Rose *et al.*, 2000; Stahl *et al.*, 2003), and degeneration of white matter tracts in frontal, temporal and parietal lobes (Bozzali *et al.*, 2001; Bozzali *et al.*, 2002; Choi *et al.*, 2005). Given that cognitive function entails the integration of different regions into a neural network for successful completion of a task, it is expected that a task demanding a high level of neuronal cooperation may be a sensitive diagnostic tool for Alzheimer's disease. This is supported by studies that suggest that Alzheimer's disease type neuropathology affects intracortical property neurons specifically (Armstrong, 1993; Mann, 1996). Assuming that interacting regions are an important prerequisite for normal cognitive function, changes in the interaction among regions of a network could precede changes in regional activation.

In the present study we tested this idea in a group of subjects with mild cognitive impairment (MCI) (Petersen *et al.*, 1999, 2001). Subjects in this group had a higher risk of conversion to Alzheimer's disease than cognitively normal subjects (Flicker *et al.*, 1991; Bowen *et al.*, 1997; Petersen *et al.*, 1999; Daly *et al.*, 2000; Ritchie *et al.*, 2001; Bennett *et al.*, 2002; Larrieu *et al.*, 2002; Palmer *et al.*, 2002; Lopez *et al.*, 2003). We have shown that in a face-matching task there were no statistically significant differences in activation between the MCI and a healthy control group (Bokde *et al.*, submitted for publication). In both groups the main peak of activation in the posterior cortex was in the right middle fusiform gyrus (FG). As the right middle FG is a key structure in the processing of face stimuli (Allison *et al.*, 1994; Puce *et al.*, 1995, 1996; Haxby *et al.*, 1996; Kanwisher *et al.*, 1997; Gauthier *et al.*, 2000; Haxby *et al.*, 2001), we investigated whether the functional connectivity of the right middle FG to the rest of the brain differs between groups. The proposed analysis addresses the need for research methodology that can detect a brain deficit before it becomes visible as a baseline condition. Functional connectivity was determined by evaluating the positive and negative interregional linear correlation coefficient between the peak activation voxel in the right FG and all other brain areas in both the MCI and healthy control groups. Functional connectivity has not been utilized previously to investigate changes in groups of subjects that may be at high risk for developing Alzheimer's disease.

Methods

Subjects

A total of 16 MCI patients and 19 healthy controls were included in the study (demographic and neuropsychological profiles are given in Table 1). The MCI patients were recruited from a specialized Alzheimer's disease clinic in the Alzheimer Memorial Center, Ludwig Maximilian University, Munich, Germany. MCI was diagnosed using the criteria established by Peterson *et al.* (1999, 2001). The diagnosis criteria were, briefly, (i) memory impairment for the age and education of the subject, (ii) normal cognitive function outside of memory and (iii) no impairment in activities of daily living. Memory complaint was corroborated by a close family member and clinical judgement was utilized to determine whether there was impairment in daily living. The threshold for determining memory impairment was 1.5 SD below the age norms (Welsh *et al.*, 1994; Berres *et al.*, 2000) in one of the three memory subtests of the CERAD neuropsychological test battery: word list memory, word list recall and word list recognition (Morris *et al.*, 1989). The neuropsychological profiles of the MCI subjects have been included as a

Table 1 Demographic and neuropsychological characteristics of the healthy control and MCI groups

	Healthy controls	MCI subjects
Number	8M/11F	8M/8F
Age	66.7 (4.2)	69.9 (7.8)
Education	12.8 (2.9)	13.2 (3.3)
MMSE [30]	29.2 (1.0)	27.2 (1.5)*
Word list memory [30]	23.9 (3.0)	15.9 (3.5)*
Word list recall [10]	8.3 (1.8)	3.8 (2.0)*
Word list recognition [10]	9.9 (0.2)	8.4 (1.6)**
Verbal fluency	24.1 (7.0)	16.7 (4.3)**
Modified Boston Naming Test [15]	14.6 (0.7)	14.1 (1.7)
Constructional praxis [11]	10.5 (0.8)	10.4 (1.0)

Values given in [ ] brackets indicate maximum possible score for each specified test except verbal fluency, for which a maximum score does not exist. Values are given as mean (standard deviation). *Statistically significant difference at the $P < 0.0001$ level. **Statistically significant difference at the $P < 0.001$ level.

supplement. The evaluation included medical, neurological, psychiatric and neuropsychological examinations; laboratory testing; EEG investigations and structural MRI. Subjects were excluded if they had cortical infarction, excessive subcortical vascular disease, space-occupying lesions, any type of dementia or any other type of disease that might impair cognitive function (e.g. major depression). The healthy controls did not have active neurological or psychiatric illness, did not have an illness that could affect cognitive function and were independently functioning members of the community. This group was recruited from the community through a local adult education programme and from partners of the MCI subjects. MCI and healthy control subjects were excluded also on factors based on MRI criteria such as pacemaker implant, metallic implants and claustrophobia. In addition, all subjects had normal vision or that corrected to the normal standard by the use of MRI-compatible eyeglasses. All subjects gave written informed consent to participate in the study after the study was explained to them. The study was performed in accordance with the Declaration of Helsinki and the Ethics Committee of the Medical Faculty of Ludwig Maximilian University approved the study.

Stimuli and task

The face-matching task consisted of two faces presented simultaneously, and participants were asked to decide on each trial whether the pair of faces was identical. If it was, the subject would respond by pressing a button in the right hand. No response was required if the pair of faces was dissimilar. The faces were grey scale stimuli where only the face was visible (ears, hair and neck were edited out). Each trial was 2.8 s long, with an interval of 0.318 s between each pair of faces. There were eight trials per block and three blocks of the task in each run, and 80% of the pairs of faces were matched pairs. The faces were obtained from the Max Planck Institute for Biological Cybernetics database (Blanz and Vetter, 1999). In the control task, the subject had to press the button every time a pair of abstract images appeared. There were four blocks of the control task and the parameters for the presentation of the images were identical to the face-matching task. There was a single run per subject. There was another task measured in each subject and the tasks were randomized across subjects. The other task is not the subject of this report.

Scanning

The imaging sequence was an interleaved T_2^*-weighted echoplanar sequence with 28 axial slices (slice thickness = 4 mm and slice gap = 1 mm, repetition time (TR) = 3.6 s, echo time (TE) = 60 ms, flip angle = 90°, field of view (FOV) = 240 mm, matrix = 64 × 64) and 69 volumes were acquired per run (each volume was measured in 2.8 s with 0.8 s gap between volumes) on a 1.5 T Siemens Magnetom Vision scanner (Erlangen, Germany). For anatomical reference in each subject, a T_1-weighted sequence with 28 slices was acquired in the same orientation as the EPI sequence (TR = 620 ms, TE = 12 ms, flip angle = 90°, FOV = 240 mm, matrix = 224 × 256, rect. FOV = 7/8, effective thickness = 1.25 mm), and a high resolution T_1-weighted 3D magnetization prepared rapid gradient echo (MPRAGE) structural image was obtained (TR = 11.4 ms, TE = 4.4 ms, flip angle = 8°, FOV = 270 mm, matrix = 224 × 256, rect. FOV = 7/8, effective thickness = 1.25 mm).

Data analysis

The data were analysed off line on a computer with an Intel Pentium III CPU (San Jose, California, USA), running Linux (Red Hat version 7.0, Red Hat Inc, Raleigh, North Carolina, USA) using AFNI (Cox, 1996) (http://afni.nimh.nih.gov/afni) and FSL (FMRIB Software Library—http://www.fmrib.ox.ac.uk/fsl).

The initial step was to delete the first four volumes of each scan to remove the initial T_1 magnetic transients in the data. The remaining data were corrected for the timing differences between each slice using Fourier interpolation. Then the data were corrected for motion effects (six-parameter rigid body), where the reference volume was in the centre of the run. Then global proportional scaling was applied to the data, the time series was high pass filtered with a filter cut-off of (1/100) Hz, the functional images were transformed to standard stereotaxic space using the structural images (as defined by the Montreal Neurological Institute/International Consortium for Brain Mapping 152 standard (MNI/ICBM), as contained within the FSL software package) and the data were smoothed using a Gaussian filter with a full width of 8 × 8 × 8 mm at half maximum. The data of each group were averaged into a single dataset to produce a mean time series. The functional connectivity at each voxel was calculated using the averaged time series. Thus, in effect we calculated the functional connectivity for the average subject in each group.

The structural images of the non-brain tissue were edited using BET first (Smith, 2002) and then edited manually for any remaining non-brain tissue on the images. The EPI images were first co-registered to the 28-slice T_1-weighted image (seven-parameter rigid body), the 28-slice T_1-weighted image was registered to the MPRAGE image (seven-parameter rigid body) and the MPRAGE image was registered to the MNI/ICBM template (12 parameter).

To determine functional connectivity the linear correlation coefficient was calculated between the time series at the location of the peak activation in the right middle FG and the rest of the brain. Because of the spatial smoothing of each voxel, a single voxel's activity can be taken as the activity of a region around that voxel. The strongest peak of activation in the right FG was located at the coordinate (40, −75, −13 mm) with a *Z*-value of 5.09 and at the coordinate (36, −71, −12 mm) with a *Z*-value of 5.37 for the MCI and healthy control groups, respectively. The difference in location of the peaks between both groups was <6 mm. We computed the linear correlation (both positive and negative) in both groups with reference to both voxel locations. We found no differences in functional connectivity within each group relative to both locations, so we have presented in this report the functional connectivity with reference to the voxel location in the healthy control group.

Statistical significance was set at the voxel level at a linear correlation coefficient value of 0.32, which corresponds to $P < 0.01$ in a time series of 65 data points. Only clusters with a minimum of 50 contiguous voxels (voxel size = 2 × 2 × 2 mm, for a minimum cluster size of 400 μl) above the threshold level were computed as statistically significant. To check whether the linear correlation was different between groups, the linear correlation coefficient was converted into *Z*-values using the Fisher Z-transformation. To compare the equality of the linear correlation coefficient between groups, a two-tailed *t*-test based on the Z-transformation was performed. Statistical significance for each voxel was set at $P < 0.01$ and each cluster size had a minimum of 50 continuous voxels above the threshold level.

The location of the activation in the brain was found with reference to the Talairach and Tournoux template (Talairach and Tournoux, 1988). To convert the MNI/ICBM coordinates to the Talairach and Tournoux coordinates, we used a non-linear transformation method developed by M. Brett for transforming

coordinate location between both stereotaxic spaces (see online at http://www.mrc-cbu.cam.ac.uk/Imaging/mnispace.html).

Results

This section contains a description of the location of the correlation coefficient peaks in the healthy control and MCI groups for the face-matching task, as well as the peaks in differences in the correlation coefficient between groups.

Neuropsychological and behavioural performance

There were statistically significant differences in the mean scores between both groups in the MMSE, word list memory, word list recall, word list recognition, and verbal fluency subtests of the CERAD battery (*see* Table 1, *t*-test, $P < 0.05$, uncorrected for multiple comparisons). In the naming and constructional praxis of the CERAD there were no statistically significant differences. The memory impairment in the MCI group was distributed across word list memory, word list recall and word list recognition. As can be seen, the MCI group had lower performance than the healthy controls in the verbal fluency subtest, even though the performance of the MCI group was within the normal range. This decrease in verbal fluency performance could indicate executive function impairment. The level of education in both in the healthy control and MCI groups was 12.8 (2) and 13.2 (3.3) years, respectively. There was no statistically significant difference in education (unpaired *t*-test, $P > 0.05$).

The performance in the face-matching task was not different statistically, with a mean correct response rate (mean and standard deviation) of 91.7 (7.2) and 87.8 (11.3) for the healthy control and MCI, respectively (*t*-test, $P > 0.05$ level). The response time was 1.53 (0.32) s and 1.46 (0.32) s for the healthy control and MCI, respectively. There was no statistically significant difference in response time between groups (*t*-test, $P > 0.05$ level). The age and gender distributions were not statistically different.

Functional connectivity in the healthy control group

There was strong linear correlation of the right middle FG with a wide network of regions in the right and left hemispheres (Table 2 and Fig. 1). The linear correlation peaks within the right hemisphere were located in cuneus, lingual gyrus, occipital gyrus, inferior and superior parietal lobule, FG, hippocampus, middle temporal gyrus (MTG), and within the frontal lobe in the inferior and middle frontal gyri and anterior cingulate gyrus. The linear correlation peaks in the left hemisphere were located in lingual gyrus, middle occipital gyrus, FG, MTG, inferior parietal lobule (IPL), and within the frontal lobe in the inferior frontal gyrus and prefrontal gyrus.

Table 2 Location of statistically significant positive functional connectivity peaks in healthy controls

Region	Brodmann area	*x*	*y*	*z*	CC
Right hemisphere					
Occipital lobe					
Cuneus	17	4	−97	3	0.66
Lingual gyrus	18	8	−72	5	0.84
Occipital gyrus	18	40	−87	3	0.94
Superior occipital gyrus	19	28	−65	31	0.89
Parietal lobe					
Inferior parietal lobule	40	50	−28	31	0.73
Superior parietal lobule	40	34	−54	49	0.94
Temporal lobe					
Fusiform gyrus	37	36	−51	−18	0.94
Middle temporal gyrus	39	36	−71	15	0.92
Hippocampus		18	−10	−13	0.72
		23	−24	−7	0.75
Frontal lobe					
Inferior frontal gyrus	47	36	27	−8	0.85
		54	23	−5	0.84
	45	38	24	19	0.89
		42	22	12	0.90
	44	42	5	27	0.93
		50	13	25	0.93
	10	34	58	3	0.73
Middle frontal gyrus	47	42	50	−9	0.79
	46	44	37	15	0.89
Anterior cingulate gyrus	32	4	23	41	0.84
Limbic system					
Thalamus		18	−29	3	0.66
Left hemisphere					
Frontal lobe					
Inferior frontal gyrus	44	−40	7	20	0.79
	47	−34	21	−4	0.74
Prefrontal gyrus	6	−44	2	30	0.81
		−34	−4	37	0.82
Parietal lobe					
Inferior parietal lobule	40	−26	−54	43	0.83
Temporal lobe					
Middle temporal gyrus	20	−44	−30	−14	0.75
Fusiform gyrus	37	−40	−55	−16	0.91
Occipital lobe					
Lingual gyrus	19	−22	−54	3	0.74
	18	−10	−74	−8	0.85
Middle occipital gyrus	37	−46	−72	−7	0.93
		−30	−25	−4	0.71
	19	−44	−81	8	0.85
		−32	−75	15	0.87
Basal ganglia					
Putamen		−20	−9	12	0.81

CC = linear correlation coefficient.

In addition, there were regions of the brain with negative linear correlation with the right middle FG. These regions were located in the right hemisphere in the superior temporal gyrus and medial frontal gyrus. In the left hemisphere there were peaks in the IPL, angular gyrus, superior frontal gyrus and anterior cingulate gyrus [*see* Table 4(a)].

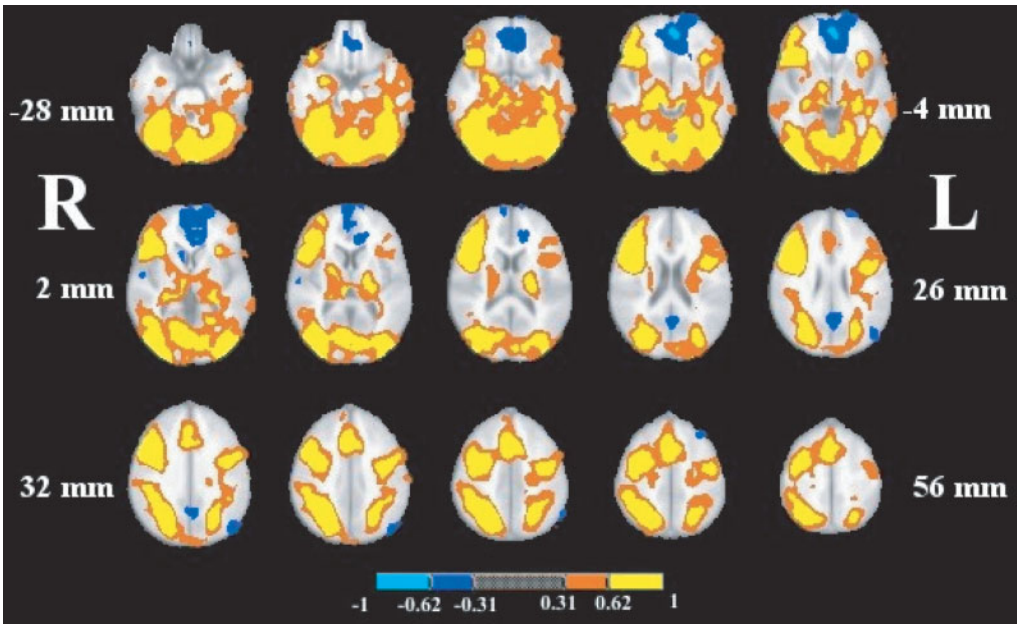

Fig. 1 Map of the regions linearly correlated with the right fusiform gyrus in healthy control.

Functional connectivity in the MCI group

The locations of the linear correlation peaks in the MCI group were as extensive as in the healthy control group (Table 3 and Fig. 2). Within the right hemisphere the peaks were located in the middle and occipital gyri, MTG, inferior and superior parietal lobule, and inferior and medial frontal gyri. The locations of the peaks in the left hemisphere were located in the cuneus, occipital gyrus, inferior and middle occipital gyri, FG, superior parietal lobule (SPL) and inferior frontal gyrus.

In addition, the MCI group had negative peaks of linear correlation within the right hemisphere in the MTG, precuneus and anterior cingulate. In the left hemisphere the peaks were located in the IPL, angular gyrus, and posterior cingulate gyrus (Table 4).

Differences in functional connectivity between MCI and healthy control groups

The areas of higher positive linear correlation in healthy controls compared with MCI subjects were located primarily in the visual processing areas of the brain (Table 5 and Fig. 3). The peaks were located within the right hemisphere in the cuneus, lingual gyrus, FG, inferior, middle and superior temporal gyrus, angular gyrus, SPL, precentral gyrus, and inferior and middle frontal gyri and cerebellum. In the left hemisphere the peaks were located in the cuneus, lingual gyrus, FG, middle occipital gyrus, inferior and middle temporal gyri, parahippocampal gyrus, angular gyrus, inferior frontal gyrus, and precentral gyrus, thalamus and cerebellum.

In particular, when examining the data on the slice at $z = -12$ mm (Fig. 3), the regions of highest positive linear correlation (yellow on the image) of the healthy control compared with the MCI was in the left FG. This indicates

Table 3 Location of statistically significant positive functional connectivity peaks in MCI

Region	Brodmann area	*x*	*y*	*z*	CC
Right hemisphere					
Occipital lobe					
Middle occipital lobe	19	34	−81	11	0.78
Superior occipital gyrus	19	22	−70	37	0.72
Temporal lobe					
Middle temporal lobe	39	30	−67	20	0.70
Parietal lobe					
Inferior parietal lobe	40	32	−50	43	0.82
		48	−33	40	0.65
Superior parietal lobe	7	22	−63	53	0.72
Frontal lobe					
Inferior frontal gyrus	47	34	23	1	0.74
	46	38	30	11	0.76
	44	44	9	2	0.82
		52	13	33	0.85
Medial frontal gyrus	8	4	33	41	0.72
Left hemisphere					
Occipital lobe					
Cuneus	17	−22	−101	2	0.73
Occipital gyrus	19	−50	−80	1	0.86
Inferior occipital gyrus	19	−42	−80	−4	0.86
Middle occipital gyrus	19	−44	−83	10	0.80
Temporal lobe					
Fusiform gyrus	37	−46	−55	−17	0.76
		−44	−53	−11	0.74
		−34	−51	−18	0.75
Parietal lobe					
Superior parietal lobule	7	−28	−54	50	0.70
Frontal lobe					
Inferior frontal gyrus	44	−52	9	29	0.71
		−37	1	27	0.74
		−38	3	20	0.72
	47	−32	23	−1	0.70

CC = linear correlation coefficient

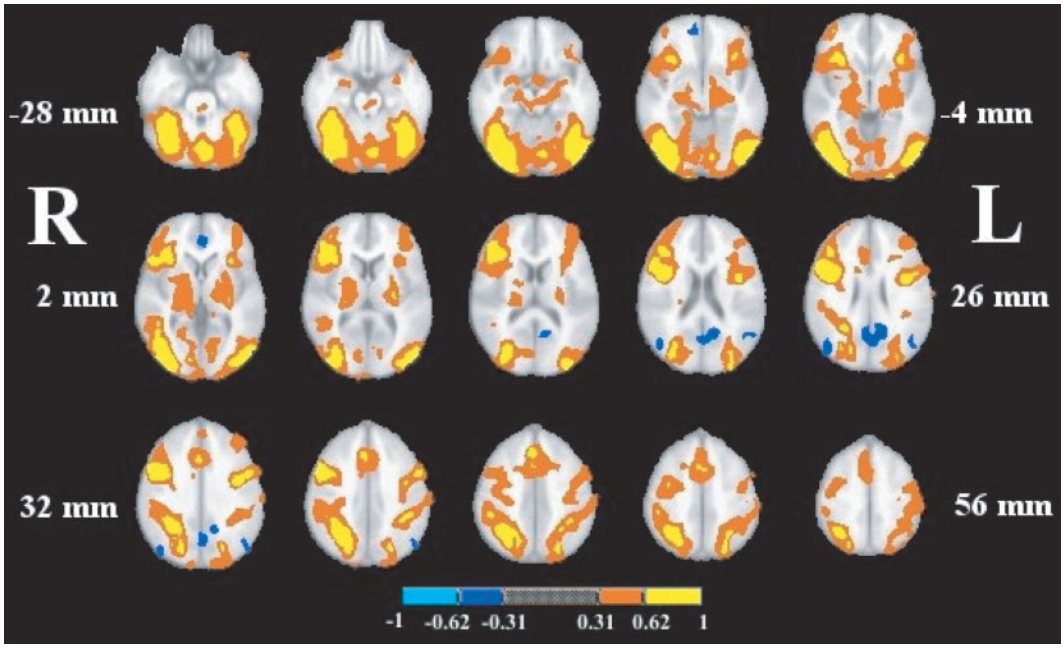

Fig. 2 Map of the regions linearly correlated with the right fusiform gyrus in MCI.

Table 4 Location of statistically significant negative functional connectivity peaks in healthy controls and MCI subjects

Region	Brodmann area	*x*	*y*	*z*	CC
Healthy controls					
Right hemisphere					
Superior temporal gyrus	22	54	−4	2	−0.51
Medial frontal gyrus	10	4	51	3	−0.65
Left hemisphere					
Superior frontal gyrus	10	−24	64	−10	−0.61
	10	−24	65	20	−0.61
Anterior cingulate gyrus	32	−8	31	−10	−0.62
	24	−8	35	−2	−0.63
Angular gyrus	39	−48	−70	31	−0.57
Inferior parietal lobule	40	−55	−56	45	−0.47
MCI subjects					
Right hemisphere					
Precuneus	31	0	−61	23	−0.60
Middle temporal gyrus	39	46	−72	29	−0.60
Anterior cingulate	32	0	43	0	−0.51
Left hemisphere					
Inferior parietal lobe	40	−54	−55	23	−0.45
Angular gyrus	39	−48	−66	37	−0.51
Posterior cingulate gyrus	31	−14	−55	27	−0.60

CC = linear correlation coefficient.

that the linear correlation between both fusiform gyri was much stronger than in the MCI group.

In the areas of positive linear correlation with the right middle FG, the MCI group had significantly higher linear correlation in the left cuneus. The increased linear correlation in MCI compared with healthy controls was located superior to the areas where the healthy control had higher positive linear correlation than the MCI group (Table 6, peaks with [+] symbol appended to *Z*-value). In the superior part of the cuneus, there was no statistically significant linear correlation in the healthy control to the right middle FG region.

Comparing the regions where either of both groups had negative linear correlations with the middle FG, we found that the healthy control group had no regions of reduced negative linear correlation (i.e. closer to zero) compared with the MCI group. The peaks of reduced negative linear correlation in the MCI group compared with the healthy control group were located in the right hemisphere in the superior temporal gyrus, anterior cingulate gyrus and

Table 5 Peaks of functional connectivity significantly higher in healthy controls than in MCI

Region	Brodmann area	x	y	z	Z-value
Right hemisphere					
Frontal lobe					
Middle frontal gyrus	6	28	6	46	5.38
		28	10	51	5.42
		46	2	44	4.84
Inferior frontal gyrus	44	48	5	13	5.57
Precentral gyrus	6	34	−6	41	4.19
Parietal lobe					
Superior parietal lobe	7	12	−57	56	4.88
Angular gyrus	39	30	−59	31	5.59
Temporal lobe					
Inferior temporal gyrus	20	68	−26	−16	4.10
		34	−8	−40	4.19
Middle temporal gyrus	39	46	−69	18	7.79
Superior temporal gyrus	38	36	15	−28	4.79
Occipital gyrus					
Cuneus	18	26	−99	9	4.09
	31	4	−77	6	4.99
Lingual gyrus	18	2	−80	1	5.09
		20	−74	4	4.92
	19	8	−56	1	4.28
Fusiform gyrus	20	28	−38	15	4.12
	37	34	−61	−5	4.17
		52	−60	−10	4.60
Cerebellum					
		6	−69	−12	4.25
		6	−60	−24	4.14
		18	−84	−40	4.21
		50	−63	−19	5.05
Left hemisphere					
Frontal lobe					
Inferior frontal gyrus	47	−55	40	−10	4.10
Precentral gyrus	9	−32	−6	41	4.57
Parietal lobe					
Angular gyrus	39	−23	−53	32	6.34
Temporal lobe					
Inferior temporal gyrus	21	−42	−21	−21	5.58
Middle temporal gyrus	21	−71	−16	−4	4.28
Parahippocampal gyrus	30	−28	−43	2	4.72
Occipital lobe					
Cuneus	17	−4	−85	12	5.08
	18	−14	−86	17	4.73
Lingual gyrus	19	−26	−54	3	4.86
		−14	−49	−3	4.43
	18	−24	−68	−3	6.79
Fusiform gyrus	37	−36	−43	−8	5.25
Middle occipital gyrus	19	−24	−75	13	5.18
Limbic system					
Thalamus		−18	−7	10	4.37
Cerebellum					
		−8	−87	−34	4.32
		−24	−51	−46	4.66
		−28	−14	−36	5.33
		−31	−64	−25	5.45

superior frontal gyrus (Table 6, peaks with [−] symbol appended to *Z*-value, and Fig. 3). In the left hemisphere the peaks were located in left IPL; anterior cingulated; and inferior, middle and superior frontal gyri. In the IPL, the MCI group had lower negative linear correlation than the healthy control group in areas posterior and/or lateral to the areas where the healthy control group had greater positive linear correlation than the MCI group.

Time series in healthy control and MCI groups

The average time series for the reference voxel in the healthy control and MCI groups, as well as the peak of functional connectivity differences in the right inferior frontal gyrus between the healthy control and MCI groups, where healthy control > MCI, was computed. The time series was averaged over the different blocks of the face-matching task and control task so that a representative time series for the control and face-matching task is obtained (*see* Fig. 4). The time series in the reference voxel (right middle FG) in both groups was very similar. The time series of the peak difference between healthy control and MCI groups showed a time series in the healthy control that had negative values during the control task and showed an increase in the magnitude during the face-matching block. In contrast, the MCI group did not show significant differences between the control task and the face-matching task. The correlation coefficient between the right middle FG and the right inferior frontal gyrus was 0.875 ($P < 0.001$) and 0.341 ($P < 0.05$) for the healthy control and MCI groups, respectively. The increase in the correlation coefficient in the healthy control group compared with the MCI group was statistically significant ($P < 0.001$).

Discussion

We have demonstrated that the right middle FG had bilateral positive linear correlation with the visual cortex in healthy control and MCI groups, in the inferior parietal lobes and in the frontal lobes. In both groups there was negative correlation between the right middle FG and inferior parietal regions and posterior cingulate, and additionally negative correlation with the medial frontal regions in the healthy control group. In addition, we found that there was statistically significant higher linear correlation of the right middle FG to the visual processing areas, the parietal lobes and right dorsolateral prefrontal cortex (DLPFC) in the healthy control group than the MCI group. The MCI group had higher positive linear correlation in the cuneus than the healthy control group, which may indicate an initial compensatory process within the MCI group. In the negatively correlated regions we found that the healthy control group had significantly lower negative linear correlation between the right middle FG and the medial frontal lobes than the MCI group. The changes in functional connectivity that we found could be the initial functional changes within the ventral visual system in MCI subjects.

The right middle FG is a key structure that was activated in both groups of subjects during the face-matching task

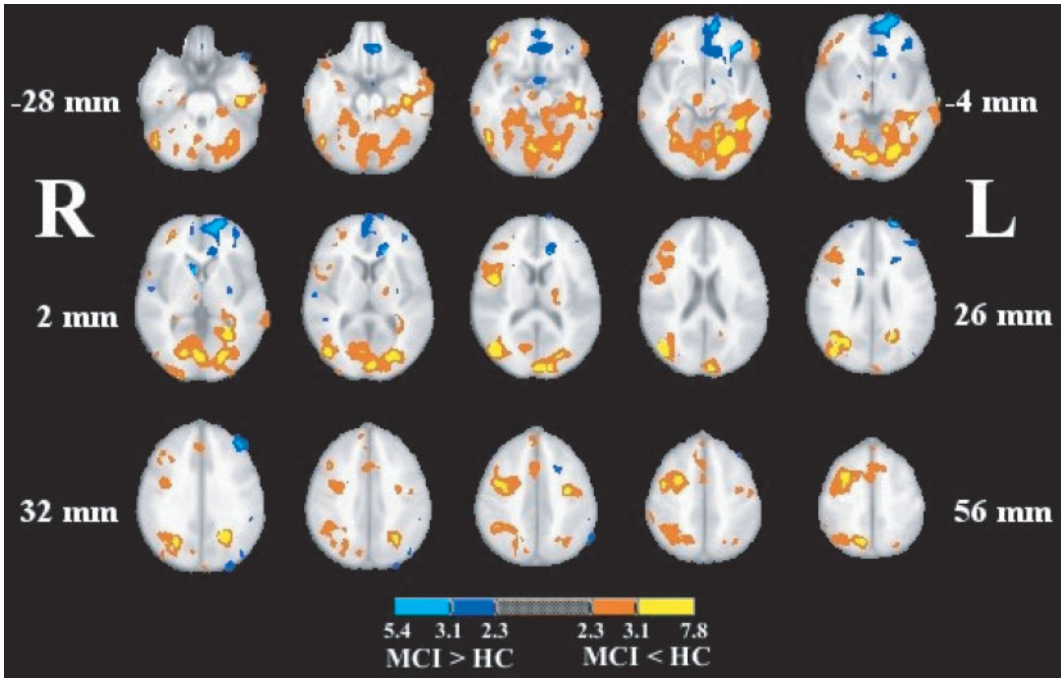

Fig. 3 Map of the regions showing statistically significant differences in the linear correlation coefficient between healthy control and MCI groups. The regions with orange/yellow overlap indicate healthy control > MCI and regions with blue/light blue overlap indicate MCI > healthy control.

Table 6 Peaks of functional connectivity significantly higher in MCI subjects than in healthy controls

Region	Brodmann area	*x*	*y*	*z*	*Z*-value
Right hemisphere					
Frontal lobe					
Superior frontal gyrus	9	19	64	23	3.76[–]
Anterior cingulate gyrus	24	20	41	9	3.30[–]
Temporal lobe					
Superior temporal gyrus	38	40	24	−28	4.13[–]
	42	52	−30	18	3.80[–]
Left hemisphere					
Frontal lobe					
Inferior frontal gyrus	47	−24	23	−10	3.78[–]
Middle frontal gyrus	9	−40	44	29	4.32[–]
	11	−30	36	−12	4.84[–]
		−8	36	−19	4.16[–]
Superior frontal gyrus	10	−24	65	21	4.83[–]
		−14	62	−7	5.37[–]
Anterior cingulate gyrus	32	−14	34	9	4.34[–]
		−24	26	23	3.33[–]
Parietal lobe					
Inferior parietal lobule	40	−59	−52	43	3.16[–]
		−55	−35	33	3.72[–]
Cuneus	19	−28	−87	36	3.14[+]
Limbic system					
Caudate nucleus		8	14	3	4.43[–]
Putamen		−24	0	−7	3.26[–]

[+] symbol indicates that the differences were due to higher positive linear correlation in the MCI group compared with the healthy control group. [–] symbol indicates that the differences were due to reduced negative correlation (closer to zero) in the MCI group compared with the healthy control group.

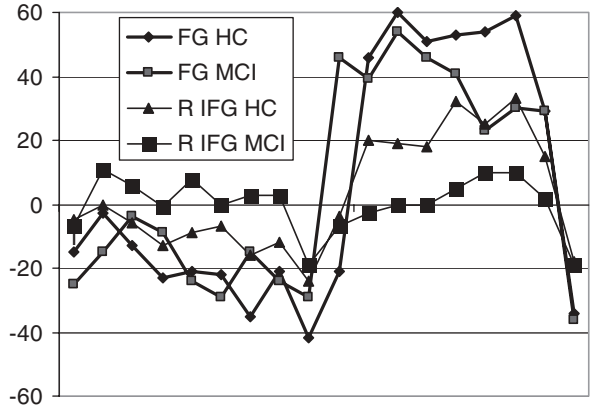

Fig. 4 Average time series of the reference voxel in the right middle FG ($x = 36$ mm, $y = -71$ mm, $z = -12$ mm) in the healthy control and MCI groups and the peak of functional connectivity differences between healthy control and MCI (where healthy control > MCI) in the right inferior frontal gyrus (IFG) ($x = 48$ mm, $y = 5$ mm, $z = 13$ mm). The individual blocks of the face-matching task and the control task have been averaged into a representative time series. The ordinate values are artificial units (AU).

(Bokde *et al.*, submitted for publication). The peak of activation in both groups was located within 6 mm. The right middle FG has been shown to contain a region specialized for processing face stimuli (referred to as the face fusiform area) (Clark *et al.*, 1996; Kanwisher *et al.*, 1997; Wojciulik *et al.*, 1998; Gauthier *et al.*, 2000; Druzgal and D'Esposito, 2001). The same level of activation in the right middle FG shows that the activation in the face fusiform area was not

degraded in the MCI group. In addition, we found that the right middle FG had higher linear correlation with the left middle FG in the healthy control group than the MCI group, an area that has been shown to also be involved in processing face stimuli (Kanwisher *et al.*, 1997; Wojciulik *et al.*, 1998; Gauthier *et al.*, 2000). The decreased functional connectivity between the FG found in the MCI group compared with the healthy control may be due to loss of input into the left middle FG. The decrease in input may be due to the presence of cholinergic lesions in MCI subjects (Mesulam *et al.*, 2004); specifically, it has been shown that cholinergic deficits exist in the primary visual cortex in mild Alzheimer's disease (Ikonomovic *et al.*, 2005). In addition, it has been shown that modulation of the cholinergic system through infusion of physostigmine in healthy subjects leads to modulation of the visual and frontal cortices, with increased activation in the visual cortex and related decrease in activation in the frontal lobes (Furey *et al.*, 1997).

In both groups the areas of the brain that were linearly correlated with the right middle FG formed an extensive network in the visual processing areas of the brain, bilaterally in the frontal lobes and parietal lobes. However, the strength of the linear correlation in the visual cortex, IPL and right DLPFC was significantly reduced in the MCI group compared with the healthy control group. The changes of functional connectivity between the right middle FG and the other regions may be one of the earliest differences in the visual cortex between the healthy control and MCI groups. A previous study investigating the activation in MCI during performance of a memory encoding task found that in the MCI group activation was decreased in the early phase of the BOLD signal within the occipital cortex compared with the healthy control group (Rombouts *et al.*, 2005). In the same study, mild Alzheimer's disease patients were shown to have differences in the early phase of the BOLD signal in the occipital lobes and also in other regions of the brain compared with the healthy control group. Further supporting that the functional connectivity changes to the visual cortex, parietal lobes and right DLPFC may be due to disease processes, Furey *et al.* (1997) have found that Alzheimer's disease patients during a working memory task using face stimuli had lower activation in the visual processing areas than the healthy controls and that the Alzheimer's disease patients relied more upon the frontal lobes while the healthy controls relied more upon the early visual processing areas for performance of the task. Horwitz *et al.* (1995), investigating functional connectivity during a face-matching task in mild Alzheimer's disease patients using positron emission tomography, found that mild Alzheimer's disease patients used a different network for performance of the task compared with age-matched healthy controls and young healthy controls.

We found that the right middle FG in the MCI group had higher positive linear correlation with the cuneus than the healthy control group. The higher linear correlations are due to the lack of functional connectivity to these regions in the healthy controls. These increases in functional connectivity could be the initial steps of a compensatory process within the MCI group. Object recognition tasks activate the ventral visual pathway in healthy controls (Corbetta *et al.*, 1990; Corbetta *et al.*, 1991; Haxby *et al.*, 1991); thus, the stronger functional connectivity in the dorsal pathway of the MCI group may indicate that it is using other regions along the dorsal visual pathway for performance of a task. The dorsal pathway has been shown to be activated in tasks requiring processing of location, colour and motion (Corbetta *et al.*, 1990; Corbetta *et al.*, 1991; Haxby *et al.*, 1991). Thus the MCI subjects may be performing the task utilizing a different strategy, one based on localization or spatial strategy to make a face comparison. It could also be the case that the MCI subjects may be utilizing the same strategy as healthy controls, but recruiting different neural networks to subserve task performance. Grady *et al.* (2001) found through the use of functional connectivity that there was recruitment of different regions of the brain for performance of delay-match to sample task, with the Alzheimer's disease patients and healthy controls recruiting different regions—in particular the amygdala was a key region activated in Alzheimer's disease patients that was not activated in healthy control. In a following study, Grady *et al.* (2003) found that mild Alzheimer's disease patients recruited a different network for a memory task and that performance of the task was correlated with activation in this network. Thus Grady *et al.* (2001, 2003) found changes in the network recruited for a memory task for Alzheimer's disease patients. In the present study, we found changes in the linear correlation between the right middle FG and visual cortex and frontal lobes, indicating changes in the functional connectivity with the entire network. An example of the manner in which the network changed is illustrated in Fig. 4, where the time series in the right inferior frontal gyrus remains approximately constant in the MCI group, while in the healthy control group the time series is phase coupled with the time series of the right middle FG. The time series in the right middle FG in the healthy control and MCI groups were very similar, so the differences in functional connectivity were not due to changes within the right FG.

In addition to the positive linear correlations, we examined negative linear correlations with the right middle FG. The right middle FG had negative linear correlation with the posterior cingulate and IPL in both groups, and with the medial frontal areas in the healthy control only. The negative linear correlation of this network with the right middle FG indicates that these regions are anti-correlated to the activation in the right middle FG and that these were suppressed during activation of the right middle FG, and thus correlated with the performance of the face-matching task. Previous studies have shown that activation of a network composed of the posterior cingulate, IPL and medial frontal areas reflect neural activity due to unconstrained verbal processes, monitoring of the external environment, body image and emotional state (Shulman *et al.*, 1997; Raichle *et al.*, 2001). When cognitive resources are focused on a task that is demanding or

novel, activity in this network is attenuated but during tasks that are not demanding or novel, or during fixation or rest periods, these regions remain active (Shulman *et al.*, 1997; Gusnard *et al.*, 2001; Raichle *et al.*, 2001; Greicius *et al.*, 2003, 2004; Greicius and Menon, 2004). This network has been referred to as the 'default' network in that it is presumably always active except during performance of goal-directed tasks (Shulman *et al.*, 1997; Raichle *et al.*, 2001). Our results support this hypothesis in that these regions, in both groups, are anti-correlated to the activation of the right middle FG. The control task in our experiment was not challenging enough, so both the healthy control and MCI groups did not attenuate the activation in the default network. The present results support and extend previous studies that have found activation of the default network in older healthy controls, MCI and Alzheimer's disease patients during a resting period (fixation) (Lustig *et al.*, 2003; Greicius *et al.*, 2004; Rombouts *et al.*, 2005). In our study we found that the default network is negatively correlated with the right middle FG and with the network activated during performance of the face-matching task.

When examining the areas with negative linear correlation, the MCI group had smaller negative (closer to zero) linear correlation than the healthy control within the medial frontal areas. We found that in these regions the difference is mainly due to strong negative linear correlations in the healthy controls and very little to no negative linear correlations in the a-MCI subjects. In addition, the other areas of negative correlation such as posterior cingulate and inferior parietal regions in both groups were not significantly different. This is consistent and extends the findings of a previous study that found differences in activation of the default network in the medial frontal areas between MCI subjects and healthy controls, with the difference mainly due to lack of activation of the default network in the MCI group (Rombouts *et al.*, 2005). Lustig *et al.* (2003) found that between Alzheimer's disease patients and age-matched healthy controls there were differences in activation of the default network in the posterior cingulate region.

The correlation of the visual cortex, parietal lobes and frontal lobes with the right middle FG may serve to integrate the activation and function of the different regions into a coherent network that subserves the face-matching task. Thus our findings suggest that there were two networks active during different parts of the scan. The network correlated with the right FG was active during the face-matching task while the default network was active during the control task. A recent study proposed that cognitive networks are organized into correlated and anti-correlated networks that may serve to differentiate between competing networks that subserve opposite cognitive functions or competing representations (Fox *et al.*, 2005). Thus the evidence that we have found supports and extends the findings of Fox and colleagues (Fox *et al.*, 2005) by noting that correlated and anti-correlated networks were present in both healthy control and MCI subjects during performance of a cognitively demanding task. In the previous work Fox and colleagues found the correlated and anti-correlated networks while subjects were under different passive states (eyes closed, eyes opened, fixation).

Even though the initial diagnosis of the MCI group was as a group suffering from memory dysfunction, the MCI group was probably a heterogeneous group composed of subjects with MCI as follows: (i) those that will convert to Alzheimer's disease in the future, (ii) those that may remain classified as MCI, (iii) those that may convert to other types of dementia or neurological diseases that cause cognitive dysfunction and (iv) those that may return to normal cognitive function. Based on previous studies it can be expected that 50–80% will be converted to Alzheimer's disease within 5 years (Tierney *et al.*, 1996; Bowen *et al.*, 1997; Petersen *et al.*, 1999; Bennett *et al.*, 2002). Follow-up of the clinical development of the subjects will allow us to better elucidate in the future the difference in activation between those MCI that are converted to Alzheimer's disease and those that are converted to other neurological or psychiatric diseases and also those that do not show cognitive decline.

The results of the current study demonstrate that other techniques such as functional connectivity can offer additional insight into the dynamics of brain activation in healthy control and patient populations. This method provides information about the covariation of brain areas with each other in time that is not captured by standard activation analyses. Similarly a study of very mild Alzheimer's disease patients and healthy controls using resting state PET data found that a multivariate technique was sensitive to changes in activation between groups whereas a voxel-by-voxel univariate technique and a region of interest analysis found no differences in activation (Scarmeas *et al.*, 2004). Thus when examining changes in brain function due to disease processes, it may be useful to examine the data not only using standard analysis techniques but also using other approaches, as demonstrated in our study.

In conclusion, mild changes in memory led to functional connectivity differences in a visual processing task in a group of MCI subjects. Thus, for early detection of disease processes it may be advantageous to investigate changes in functional connectivity, as it may be a sensitive marker for disease presence.

Acknowledgements

This study was supported by a grant from the Volkswagen Stiftung (Hannover, Germany) to A.B., S.J.T. and H.H., and by a grant from the German Competency Network on Dementias (Kompetenznetz Demenzen) funded by the Bundesministerium für Bildung und Forschung.

References

Alexander GE, Chen K, Pietrini P, Rapoport SI, Reiman EM. Longitudinal PET evaluation of cerebral metabolic decline in dementia: a potential outcome measure in Alzheimer's disease treatment studies. Am J Psychiatry 2002; 159: 738–45.

Allison T, Ginter H, McCarthy G, Nobre AC, Puce A, Luby M, et al. Face recognition in human extrastriate cortex. J Neurophysiol 1994; 71: 821–5.

Armstrong RA. Is the clustering of neurofibrillary tangles in Alzheimer's patients related to the cells of origin of specific cortico-cortical projections? Neurosci Lett 1993; 160: 57–60.

Azari NP, Pettigrew KD, Schapiro MB, et al. Early detection of Alzheimer's disease: a statistical approach using positron emission tomographic data. J Cereb Blood Flow Metab 1993; 13: 438–47.

Backman L, Almkvist O, Nyberg L, Andersson J. Functional changes in brain activity during priming in Alzheimer's disease. J Cogn Neurosci 2000; 12: 134–41.

Bennett DA, Wilson RS, Schneider JA, Evans DA, Beckett LA, Aggarwal NT, et al. Natural history of mild cognitive impairment in older persons. Neurology 2002; 59: 198–205.

Berres M, Monsch AU, Bernasconi F, Thalmann B, Stahelin HB. Normal ranges of neuropsychological tests for the diagnosis of Alzheimer's disease. Stud Health Technol Inform 2000; 77: 195–9.

Blanz V, Vetter T. A morphable model for the synthesis of 3D faces. In: 26th International Conference on Computer Graphics and Interactive Techniques. Los Angeles, California, USA: ACM; 1999.

Bookheimer SY, Strojwas MH, Cohen MS, Saunders AM, Pericak-Vance MA, Mazziotta JC, et al. Patterns of brain activation in people at risk for Alzheimer's disease. N Engl J Med 2000; 343: 450–6.

Bowen J, Teri L, Kukull W, McCormick W, McCurry SM, Larson EB. Progression to dementia in patients with isolated memory loss. Lancet 1997; 349: 763–5.

Bozzali M, Franceschi M, Falini A, Pontesilli S, Cercignani M, Magnani G, et al. Quantification of tissue damage in Alzheimer's disease using diffusion tensor and magnetization transfer MRI. Neurology 2001; 57: 1135–7.

Bozzali M, Falini A, Franceschi M, Cercignani M, Zuffi M, Scotti G, et al. White matter damage in Alzheimer's disease assessed in vivo using diffusion tensor magnetic resonance imaging. J Neurol Neurosurg Psychiatry 2002; 72: 742–6.

Caselli RJ, Graff-Radford NR, Reiman EM, Weaver A, Osborne D, Lucas J, et al. Preclinical memory decline in cognitively normal apolipoprotein E-epsilon4 homozygotes. Neurology 1999; 53: 201–7.

Chetelat G, Desgranges B, de la Sayette V, Viader F, Eustache F, Baron JC. Mild cognitive impairment: can FDG-PET predict who is to rapidly convert to Alzheimer's disease? Neurology 2003; 60: 1374–7.

Choi SJ, Lim KO, Monteiro I, Reisberg B. Diffusion tensor imaging of frontal white matter microstructure in early Alzheimer's disease: a preliminary study. J Geriatr Psychiatry Neurol 2005; 18: 12–9.

Clark VP, Keil K, Maisog JM, Courtney S, Ungerleider LG, Haxby JV. Functional magnetic resonance imaging of human visual cortex during face matching: a comparison with positron emission tomography. Neuroimage 1996; 4: 1–15.

Corbetta M, Miezin FM, Dobmeyer S, Shulman GL, Petersen SE. Attentional modulation of neural processing of shape, color, and velocity in humans. Science 1990; 248: 1556–9.

Corbetta M, Miezin FM, Dobmeyer S, Shulman GL, Petersen SE. Selective and divided attention during visual discriminations of shape, color, and speed: functional anatomy by positron emission tomography. J Neurosci 1991; 11: 2383–402.

Cox RW. AFNI: software for analysis and visualization of functional magnetic resonance neuroimages. Comput Biomed Res 1996; 29: 162–73.

Daly E, Zaitchik D, Copeland M, Schmahmann J, Gunther J, Albert M. Predicting conversion to Alzheimer disease using standardized clinical information. Arch Neurol 2000; 57: 675–80.

De Santi S, de Leon MJ, Rusinek H, Convit A, Tarshish CY, Roche A, et al. Hippocampal formation glucose metabolism and volume losses in MCI and Alzheimer's disease. Neurobiol Aging 2001; 22: 529–39.

Druzgal TJ, D'Esposito M. A neural network reflecting decisions about human faces. Neuron 2001; 32: 947–55.

Flicker C, Ferris SH, Reisberg B. Mild cognitive impairment in the elderly: predictors of dementia. Neurology 1991; 41: 1006–9.

Fox MD, Snyder AZ, Vincent JL, Corbetta M, Van Essen DC, Raichle ME. From the cover: the human brain is intrinsically organized into dynamic, anticorrelated functional networks. Proc Natl Acad Sci USA 2005; 102: 9673–8.

Furey ML, Pietrini P, Haxby JV, Alexander GE, Lee HC, VanMeter J, et al. Cholinergic stimulation alters performance and task-specific regional cerebral blood flow during working memory. Proc Natl Acad Sci USA 1997; 94: 6512–6.

Gauthier I, Tarr MJ, Moylan J, Skudlarski P, Gore JC, Anderson AW. The fusiform 'face area' is part of a network that processes faces at the individual level. J Cogn Neurosci 2000; 12: 495–504.

Grady CL, Furey ML, Pietrini P, Horwitz B, Rapoport SI. Altered brain functional connectivity and impaired short-term memory in Alzheimer's disease. Brain 2001; 124: 739–56.

Grady CL, McIntosh AR, Beig S, Keightley ML, Burian H, Black SE. Evidence from functional neuroimaging of a compensatory prefrontal network in Alzheimer's disease. J Neurosci 2003; 23: 986–93.

Greicius MD, Menon V. Default-mode activity during a passive sensory task: uncoupled from deactivation but impacting activation. J Cogn Neurosci 2004; 16: 1484–92.

Greicius MD, Krasnow B, Reiss AL, Menon V. Functional connectivity in the resting brain: a network analysis of the default mode hypothesis. Proc Natl Acad Sci USA 2003; 100: 253–8.

Greicius MD, Srivastava G, Reiss AL, Menon V. Default-mode network activity distinguishes Alzheimer's disease from healthy aging: evidence from functional MRI. Proc Natl Acad Sci USA 2004; 101: 4637–42.

Grundman M, Petersen RC, Ferris SH, Thomas RG, Aisen PS, Bennett DA, et al. Mild cognitive impairment can be distinguished from Alzheimer disease and normal aging for clinical trials. Arch Neurol 2004; 61: 59–66.

Gusnard DA, Akbudak E, Shulman GL, Raichle ME. Medial prefrontal cortex and self-referential mental activity: relation to a default mode of brain function. Proc Natl Acad Sci USA 2001; 98: 4259–64.

Haxby JV, Grady CL, Horwitz B, Ungerleider LG, Mishkin M, Carson RE, et al. Dissociation of object and spatial visual processing pathways in human extrastriate cortex. Proc Natl Acad Sci USA 1991; 88: 1621–5.

Haxby JV, Ungerleider LG, Horwitz B, Maisog JM, Rapoport SI, Grady CL. Face encoding and recognition in the human brain. Proc Natl Acad Sci USA 1996; 93: 922–7.

Haxby JV, Gobbini MI, Furey ML, Ishai A, Schouten JL, Pietrini P. Distributed and overlapping representations of faces and objects in ventral temporal cortex. Science 2001; 293: 2425–30.

Herholz K, Salmon E, Perani D, Baron JC, Holthoff V, Frolich L, et al. Discrimination between Alzheimer dementia and controls by automated analysis of multicenter FDG PET. Neuroimage 2002; 17: 302–16.

Horwitz B, McIntosh AR, Haxby JV, Furey M, Salerno JA, Schapiro MB, et al. Network analysis of PET-mapped visual pathways in Alzheimer type dementia. Neuroreport 1995; 6: 2287–92.

Ikonomovic MD, Mufson EJ, Wuu J, Bennett DA, DeKosky ST. Reduction of choline acetyltransferase activity in primary visual cortex in mild to moderate Alzheimer's disease. Arch Neurol 2005; 62: 425–30.

Kanwisher N, McDermott J, Chun MM. The fusiform face area: a module in human extrastriate cortex specialized for face perception. J Neurosci 1997; 17: 4302–11.

Larrieu S, Letenneur L, Orgogozo JM, Fabrigoule C, Amieva H, Le Carret N, et al. Incidence and outcome of mild cognitive impairment in a population-based prospective cohort. Neurology 2002; 59: 1594–9.

Lopez OL, Jagust WJ, Dulberg C, Becker JT, DeKosky ST, Fitzpatrick A, et al. Risk factors for mild cognitive impairment in the Cardiovascular Health Study Cognition Study: part 2. Arch Neurol 2003; 60: 1394–9.

Lustig C, Snyder AZ, Bhakta M, O'Brien KC, McAvoy M, Raichle ME, et al. Functional deactivations: change with age and dementia of the Alzheimer type. Proc Natl Acad Sci USA 2003; 100: 14504–9.

Mann DM. Pyramidal nerve cell loss in Alzheimer's disease. Neurodegeneration 1996; 5: 423–7.

Mesulam M, Shaw P, Mash D, Weintraub S. Cholinergic nucleus basalis tauopathy emerges early in the aging-MCI-Alzheimer's disease continuum. Ann Neurol 2004; 55: 815–28.

Minoshima S, Giordani B, Berent S, Frey KA, Foster NL, Kuhl DE. Metabolic reduction in the posterior cingulate cortex in very early Alzheimer's disease. Ann Neurol 1997; 42: 85–94.

Morris JC, Heyman A, Mohs RC, Hughes JP, van Belle G, Fillenbaum G, et al. The Consortium to Establish a Registry for Alzheimer's Disease (CERAD). Part I. Clinical and neuropsychological assessment of Alzheimer's disease. Neurology 1989; 39: 1159–65.

Palmer K, Wang HX, Backman L, Winblad B, Fratiglioni L. Differential evolution of cognitive impairment in nondemented older persons: results from the Kungsholmen Project. Am J Psychiatry 2002; 159: 436–42.

Petersen RC, Smith GE, Waring SC, Ivnik RJ, Tangalos EG, Kokmen E. Mild cognitive impairment: clinical characterization and outcome. Arch Neurol 1999; 56: 303–8.

Petersen RC, Stevens JC, Ganguli M, Tangalos EG, Cummings JL, DeKosky ST. Practice parameter: early detection of dementia: mild cognitive impairment (an evidence-based review): Report of the Quality Standards Subcommittee of the American Academy of Neurology. Neurology 2001; 56: 1133–42.

Pietrini P, Furey ML, Graff-Radford N, Freo U, Alexander GE, Grady CL, et al. Preferential metabolic involvement of visual cortical areas in a subtype of Alzheimer's disease: clinical implications. Am J Psychiatry 1996; 153: 1261–8.

Puce A, Allison T, Gore JC, McCarthy G. Face-sensitive regions in human extrastriate cortex studied by functional MRI. J Neurophysiol 1995; 74: 1192–9.

Puce A, Allison T, Asgari M, Gore JC, McCarthy G. Differential sensitivity of human visual cortex to faces, letterstrings, and textures: a functional magnetic resonance imaging study. J Neurosci 1996; 16: 5205–15.

Raichle ME, MacLeod AM, Snyder AZ, Powers WJ, Gusnard DA, Shulman GL. A default mode of brain function. Proc Natl Acad Sci USA 2001; 98: 676–82.

Reiman EM, Caselli RJ, Chen K, Alexander GE, Bandy D, Frost J. Declining brain activity in cognitively normal apolipoprotein E epsilon 4 heterozygotes: a foundation for using positron emission tomography to efficiently test treatments to prevent Alzheimer's disease. Proc Natl Acad Sci USA 2001; 98: 3334–9.

Reiman EM, Chen K, Alexander GE, Caselli RJ, Bandy D, Osborne D, et al. Functional brain abnormalities in young adults at genetic risk for late-onset Alzheimer's dementia. Proc Natl Acad Sci USA 2004; 101: 284–9.

Ritchie K, Artero S, Touchon J. Classification criteria for mild cognitive impairment: a population-based validation study. Neurology 2001; 56: 37–42.

Rombouts SA, Barkhof F, Veltman DJ, Machielsen WC, Witter MP, Bierlaagh MA, et al. Functional MR imaging in Alzheimer's disease during memory encoding. AJNR Am J Neuroradiol 2000; 21: 1869–75.

Rombouts SA, Barkhof F, Goekoop R, Stam CJ, Scheltens P. Altered resting state networks in mild cognitive impairment, and mild Alzheimer's disease: an fMRI study. Hum Brain Mapp 2005; 26: 231–9.

Rombouts SA, Goekoop R, Stam CJ, Barkhof F, Scheltens P. Delayed rather than decreased BOLD response as a marker for early Alzheimer's disease. Neuroimage 2005; 26: 1078–85.

Rose SE, Chen F, Chalk JB, Zelaya FO, strugnell WE, Benson M, et al. Loss of connectivity in Alzheimer's disease: an evaluation of white matter tract integrity with colour coded MR diffusion tensor imaging. J Neurol Neurosurg Psychiatry 2000; 69: 528–30.

Scarmeas N, Habeck CG, Zarahn E, Anderson KE, Park A, Hilton J, et al. Covariance PET patterns in early Alzheimer's disease, and subjects with cognitive impairment but no dementia: utility in group discrimination, and correlations with functional performance. Neuroimage 2004; 23: 35–45.

Shulman GL, Fiez JA, Corbetta M, Buckner RL, Miezin FM, Raichle ME, et al. Common blood flow decreases across visual tasks: II. Decreases in cerebral cortex. J Cogn Neurosci 1997; 9: 648–63.

Silverman DH, Gambhir SS, Huang HW, Schwimmer J, Kim S, Small GW, et al. Evaluating early dementia with, and without assessment of regional cerebral metabolism by PET: a comparison of predicted costs, and benefits. J Nucl Med 2002; 43: 253–66.

Small GW, Ercoli LM, Silverman DH, Huang SC, Komo S, Bookheimer SY, et al. Cerebral metabolic, and cognitive decline in persons at genetic risk for Alzheimer's disease. Proc Natl Acad Sci USA 2000; 97: 6037–42.

Smith SM. Fast robust automated brain extraction. Hum Brain Mapp 2002; 17: 143–55.

Stahl R, Dietrich O, Teipel S, Hampel H, Reiser MF, Schoenberg SO. [Assessmement of axonal degeneration on Alzheimer's disease with diffusion tensor MRI]. Radiologe 2003; 43: 566–75.

Talairach J, Tournoux P. Co-planar stereotaxic atlas of the human brain. New York: Thieme Medical; 1988.

Tierney MC, Szalai JP, Snow WG, Fisher RH, Nores A, Nadon G, et al. Prediction of probable Alzheimer's disease in memory-impaired patients: a prospective longitudinal study. Neurology 1996; 46: 661–5.

Welsh KA, Butters N, Mohs RC, Beekly D, Edland S, Fillenbaum G, et al. The Consortium to Establish a Registry for Alzheimer's Disease (CERAD). Part V. A normative study of the neuropsychological battery. Neurology 1994; 44: 609–14.

Wojciulik E, Kanwisher N, Driver J. Covert visual attention modulates face-specific activity in the human fusiform gyrus: fMRI study. J Neurophysiol 1998; 79: 1574–8.